DE GRUYTER OPEN

Acta Geophysica
vol. 63, no. 6, Dec. 2015, pp. 1609-1638
DOI: 10.2478/s11600-014-0258-x

Intercomparison of Surface Energy Fluxes Estimates from the FEST-EWB and TSEB Models over the Heterogeneous REFLEX 2012 Site (Barrax, Spain)

Chiara CORBARI[1], Wim TIMMERMANS[2], and Ana ANDREU[3]

[1]Politecnico di Milano, Department of Civil and Environmental Engineering, Milano, Italy; e-mail: chiara.corbari@polimi.it (corresponding author)

[2]University of Twente, Faculty of Geo-information Science and Earth Observation, Department of Water Resources, Enschede, The Netherlands
e-mail: w.j.timmermans@utwente.nl

[3]Instituto de Investigación y Formación Agraria y Pesquera (IFAPA), Sevilla, Spain
e-mail: ana.andreu.mendez@juntadeandalucia.es

A b s t r a c t

An intercomparison between the Energy Water Balance model (FEST-EWB) and the Two-Source Energy Balance model (TSEB) is performed over a heterogeneous agricultural area. TSEB is a residual model which uses Land Surface Temperature (LST) from remote sensing as a main input parameter so that energy fluxes are computed instantaneously at the time of data acquisition. FEST-EWB is a hydrological model that predicts soil moisture and the surface energy fluxes on a continuous basis. LST is then a modelled variable. Ground and remote sensing data from the Regional Experiments For Land-atmosphere Exchanges (REFLEX) campaign in 2012 in Barrax gave the opportunity to validate and compare spatially distributed energy fluxes. The output of both models matches the ground observations quite well. However, a spatial analysis reveals significant differences between the two approaches for latent and sensible heat fluxes over relatively small fields characterized by high heterogeneity in vegetation cover.

Key words: energy balance model, water and energy balance model, remote sensing.

1. INTRODUCTION

Evapotranspiration (*ET*) is one of the most important variables in many fields such as hydrology, climatology, forest agronomy and plant physiology, and the partitioning between sensible (*H*) and latent (*LE*) heat fluxes is fundamental for the definition of crop water requirements. For irrigation practices, near-real time knowledge on soil water availability at the local and regional scale is of extreme importance in areas characterized by water scarcity.

In the past years a large number of land surface models, often called Soil-Vegetation-Atmosphere Transfer Schemes (SVAT), have been developed. However, approaches with substantial differences are included. Two main categories can be identified.

The first category concerns the so-called residual approaches which use Land Surface Temperature (LST) from remote sensing as their main input parameter. As such, energy fluxes are computed instantaneously at the time of data acquisition. Extrapolation to daily estimates, necessary for operational irrigation practice or proper water management, is generally performed by either the use of the concept of constant evaporative fraction (*i.e.*, $LE/(LE + H)$) or by using a higher temporal sampling (Chehbouni *et al.* 2008). The residual approaches are usually divided in one-source and two-source schemes, depending on the differentiation of the vegetation and bare soil contribution to the energy fluxes or treating them in a lumped manner. The Surface Energy Balance Model (SEBAL; Bastiaanssen *et al.* 1998), the Surface Energy Balance System (SEBS; Su 2002), and the Simplified Surface Energy Balance Index (S-SEBI; Roerink *et al.* 2000) treat the soil and vegetation contribution in a lumped manner, whereas the Two-Source Energy Balance (TSEB; Norman *et al.* 1995) is an example of the so-called dual source approach.

The second category of models includes coupled energy water balance schemes that predict soil moisture dynamics and usually river runoff as well as the surface energy fluxes on a continuous basis. Therefore, they are usually more complex and over-parameterized and LST is then a modelled variable instead of an input variable. Examples of these models are the Variable Infiltration Capacity (VIC) (Liang *et al.* 1994), the TOPmodel based Land Atmosphere Transfer Scheme (TOPLATS) (Famiglietti and Wood 1994), the Common Land model (CLM) (Dai *et al.* 2003), and the Flash-flood Event-based Spatially-distributed rainfall-runoff Transformation – Energy Water Balance (FEST-EWB) (Corbari *et al.* 2011). These types of model can overcome the limitations related to cloud coverage typical of thermal infrared satellite images and moreover provide continuous estimates of evapotranspiration and also of soil moisture. Of course, some limitations are present in

these models linked to the modelling of irrigation, lateral flows and groundwater, which are difficult to parameterize. Another limitation is the need of many hydraulic soil input parameters that are often not easily available at large scales, nor at high spatial resolution, even though they have an important role in the computation of the principal mass and energy fluxes.

Among the models that need remotely sensed LST as an input, a discussion is open in literature between the reliability of one-source or two-source models. In fact, in areas with sparse vegetation, a two-source model shows better performance as compared to a one-source model. However, different authors have found that with a proper calibration even a one-source model can correctly reproduce the energy fluxes (Bastiaanssen *et al.* 1998, Kustas *et al.* 1996) although a local calibration is not always possible (Su *et al.* 2001, Kustas *et al.* 2006, Cammalleri *et al.* 2012). Model suitability generally is a trade-off between easiness in use and data availability on one hand and required accuracy on the other hand.

Distributed hydrological models are usually more complex and over-parameterized with respect to remote sensing based SVAT models. This requires an accurate calibration procedure that generally depends on comparison between simulated and observed discharges at the available river cross-sections (Famiglietti and Wood 1994, Brath *et al.* 2004, Rabuffetti *et al.* 2008). Nowadays, little efforts have been focused on understanding whether remotely sensed LST can be used to calibrate and validate hydrological models parameters (Franks and Beven 1999, Crow *et al.* 2003, Gutmann and Small 2010, Corbari and Mancini 2013, Corbari *et al.* 2015).

Both types of models have been extensively validated in different climatic and soil/vegetation conditions against ground and/or remotely sensed data. However, few intercomparisons between energy balance models are made that quantify model reliability in evapotranspiration estimation in areas with heterogeneous vegetation and soil moisture conditions (Gonzalez-Dugo *et al.* 2009, Timmermans *et al.* 2007, French *et al.* 2005) or between hydrological models (Wood *et al.* 1998). Even less studies have compared these two types of models that both predict energy fluxes (Crow *et al.* 2005, Corbari *et al.* 2013), most probably due to the rather different methodologies used. The study of Crow *et al.* (2008) also tried to integrate these two types of models through assimilation of one into the other.

Most of the validation experiments usually demonstrate that these models produce reliable energy fluxes compared to ground measurements, but their accuracy at a regional scale is more difficult to demonstrate. It is therefore difficult to select the most suitable model for energy flux predictions which increases the need for further comparisons between different types of models.

In this paper, energy fluxes from a two-source model based on remotely sensed LST (TSEB) and from a continuous distributed hydrological model based on coupled water and energy balances (FEST-EWB) are compared in a spatial manner to understand their reliability and differences under different soil moisture and vegetation conditions. Both models are also validated against ground observed energy fluxes from eddy covariance stations and a scintillometer.

The area used for this comparison is the agricultural test site of Barrax (Spain) where the so-called Regional Experiments For Land-atmosphere Exchanges (REFLEX) campaign is carried out. In this framework an extensive amount of ground and airborne data have been acquired during the second half of July 2012.

The objective of this paper is to evaluate the reliability of each model and an attempt to understand under which vegetation and soil moisture conditions each model works better, given the relevant differences in the computation schemes.

2. MODELS DESCRIPTION

The FEST-EWB and TSEB models use different approaches to calculate surface energy fluxes which will be described in details in the following sections. FEST-EWB is a continuous energy and water balance model (Corbari *et al.* 2011), while TSEB, as originally formulated (Norman *et al*. 1995), is a two-source energy balance model designed for the use with instantaneous remote sensing observations.

2.1 FEST-EWB

FEST-EWB is a distributed hydrological energy water balance model (Corbari *et al.* 2010, 2011, 2013a) developed from the FEST-WB model (Mancini 1990, Rabuffetti *et al.* 2008). FEST-EWB computes the main processes of the hydrological cycle: evapotranspiration, infiltration, surface runoff, flow routing, subsurface flow (Ravazzani *et al.* 2011), snow dynamics (Corbari *et al.* 2009). The computation domain is discretized with a mesh of regular square cells in which every parameter is defined or calculated.

The input requirements (Table 1) of the model are comprised of:

- meteorological variables,
- distributed soil and vegetation parameters,
- a Digital Elevation Model (DEM),
- a Landuse/landcover map.

The core of the model is the system between the water and energy balance equations (Eqs. 1 and 2 below) which are linked through evapotranspiration. In short, the energy balance is solved by looking for a Representative

Equilibrium Temperature (RET), that is, the land surface temperature that closes the energy balance equation. This equilibrium surface temperature, which is an internal model variable, is comparable to the land surface temperature as retrieved from remote sensing data.

The soil moisture evolution for a given cell at position *i,j* is described by the energy and water balance equations:

$$\begin{cases} Rn_{i,j} - G_{i,j} - H_{i,j} - LE_{i,j} = 0\,, & (1) \\ \dfrac{\partial SM_{i,j}}{\partial t} = \dfrac{1}{dz_{i,j}}\left(P_{i,j} - R_{i,j} - PE_{i,j} - ET_{i,j}\right), & (2) \end{cases}$$

where P is the precipitation rate [mm h^{-1}], R is the runoff flux [mm h^{-1}], PE is the drainage flux [mm h^{-1}], ET is the evapotranspiration rate [mm h^{-1}], z is the soil depth [m], Rn [W m^{-2}] is the net radiation, G [W m^{-2}] is the soil heat flux, H [W m^{-2}], and LE [W m^{-2}] are, respectively, the sensible heat and latent heat fluxes. All these terms of the system are functions of the input soil and vegetation parameters.

In particular, ET is linked to the latent heat flux through the latent heat of vaporization (λ) and the water density (ρ_w):

$$LE = \lambda \rho_w ET\,. \tag{3}$$

The latent heat flux, as reported in Corbari *et al.* (2011), is then computed as

$$LE = \frac{\rho_a c_p}{\gamma}\left(e^* - e_a\right)\left[\frac{f_v}{(r_a + r_c)} + \frac{1 - f_v}{(r_{abs} + r_{\mathrm{soil}})}\right]\,, \tag{4}$$

where ρ_a is the air density, γ is the psychometric constant [Pa° C^{-1}], f_v is the vegetation fraction, and c_p is the specific heat of humid air [MJ kg^{-1} K^{-1}]. The saturation vapour pressure (e^*) is computed as a function of RET (Brutsaert 2005) and the vapour pressure (e_a) is a function of air temperature. The canopy resistance (r_c) is expressed following Jarvis (1976), while the soil resistance (r_{soil}) follows Sun (1982). The aerodynamic resistance (r_a for vegetation and r_{abs} for bare soil) is computed using the model from Thom (1975).

The sensible heat flux is computed as

$$H = \rho_a c_p \left(\mathrm{RET} - T_a\right)\left[\frac{(1 - f_v)}{r_{abs}} + \frac{f_v}{r_a}\right]\,, \tag{5}$$

where T_a is the air temperature [K].

The net radiation is computed as the algebraic sum of the incoming and outgoing short wave and long wave radiation:

$$Rn = R_s(1 - \alpha) + \varepsilon_s \varepsilon_c \sigma(T_a^4) - \varepsilon_s \sigma(\mathrm{RET}^4)\,, \tag{6}$$

where R_s is the incoming shortwave radiation [W m^{-2}], α is albedo, ε_c is the atmosphere emissivity, ε_s is the surface emissivity, and σ is the Stefan–Boltzmann constant [W m^{-2} K^{-4}].

The soil heat flux is the heat exchanged by conduction with the sub-surface soil and it is evaluated as

$$G = \left(\lambda / dz\right)\left(\mathrm{RET} - T_{\mathrm{soil}}\right), \tag{7}$$

where λ is soil thermal conductivity [W m^{-1} K^{-1}] and T_{soil} is soil temperature [K] at 10 cm depth (McCumber and Pielke 1981).

All the terms of the energy balance depend on RET, so the energy balance equation can be solved by looking for the thermodynamic equilibrium temperature that closes the equation. A Newton–Raphson scheme is used to solve this iteration process.

FEST-EWB was previously validated against energy and mass exchange measurements acquired by an eddy covariance station (Corbari *et al.* 2011) and also against ground and remote sensing information at agricultural district scale (Corbari *et al.* 2010).

2.2 The Two-Source Energy Balance (TSEB)

The Two-Source Energy Balance (TSEB), model of Norman *et al.* (1995) and Kustas and Norman (1999) has shown good performances for a wide range of arid and partially-vegetated landscapes (Timmermans *et al*. 2007, Gonzalez-Dugo 2009). Under such circumstances, a dual source model that distinguishes between the soil and vegetation contribution to the turbulent fluxes has clear and well-known advantages over simpler single-source models that treat these contributions in a lumped manner (Huntingford *et al.* 1995, Kustas *et al.* 1996). In the current contribution, the so-called series parameterization version of TSEB (Norman *et al.* 1995) is followed, allowing the interaction between soil and canopy. The input requirements of the model are summarized in Table 1.

The model assumes that the surface radiometric temperature (T_{RAD}) is a combination of soil (T_S) and canopy (T_C) temperatures, weighted by the vegetation fraction:

$$T_R(\phi) = \left\{ f_v(\phi) T_C^4 + \left[1 - f_v(\phi)\right] T_S^4 \right\}^{1/4}, \tag{8}$$

where f_v is affected by the sensor viewing angle (ϕ). The surface energy-balance equation can be formulated for the whole soil-canopy-atmosphere system, or for the soil and canopy components separately:

$$Rn_c = LE_c + H_c, \tag{9}$$

Table 1

The input requirements of the FEST-EWB and TSEB models

Observation	FEST-EWB	TSEB
Air temperature [K]	x	x
Windspeed [m s^{-1}]	x	x
Air pressure [mbar]	x	x
Relative humidity [–]	x	x
R_S [W m^{-2}]	x	x
Irrigation volume	x	
Sensor viewing angle [°]		x
NDVI (fCover, LAI)	x	x
Surface temperature		x
Emissivity	x	x
Landcover or aerodynamic properties	x	x
Soil parameters (saturated hydraulic conductivity, field capacity, wilting point, residual and saturated soil water content, soil depth)	x	

$$Rn_S = LE_S + H_S + G\,. \tag{10}$$

The original formulations for Rn, Rn_c, Rn_s, and G can be found in Norman *et al.* (1995) and Kustas and Norman (1999). Since the radiation formulation follows the so-called "layer-approach" (Lhomme and Chehbouni 1999), a simple summation of the soil and canopy components yields the total flux

$$Rn = Rn_c + Rn_s\,, \tag{11}$$

$$H = H_c + H_s\,, \tag{12}$$

$$LE = LE_c + LE_s\,. \tag{13}$$

The model is developed originally for uniformly distributed crops. In the case of clumped canopies with partial vegetation cover, such as vineyards and orchards, the parameterizations are corrected by the so-called clumping factor (Anderson *et al.* 2005). This factor corrects for the reduction in the extinction of the radiation in a clumped canopy as compared to a uniformly distributed one. The soil heat flux is then estimated as a time-dependent function of the net radiation reaching the soil, following:

$$G = c_g\, Rn_s\,, \tag{14}$$

where c_g is slightly variable with time. Details on the original determination can be found in Kustas *et al*. (1998). However, here it is calibrated *versus* local observations using the measurements from the test sites (see Section 4.1.2).

Within the series resistance scheme, the sensible heat fluxes H_c, H_s, and H are expressed as

$$H_c = \rho_a c_p (T_C - T_{AC}) / r_x \,, \tag{15}$$

$$H_s = \rho_a c_p (T_S - T_{AC}) / r_s \,, \tag{16}$$

$$H = H_s + H_c = H_c = \rho_a c_p (T_{AC} - T_a) / r_a \,, \tag{17}$$

where T_{AC} is the air temperature in the canopy air space [K], r_x is the resistance to heat flow of the vegetation leaf boundary layer [s m^{-1}], r_s is the resistance to the heat flow in the boundary layer above the soil [s m^{-1}], whereas r_a is the aerodynamic resistance calculated from the stability corrected temperature profile equations (Brutsaert 1982), using Monin-Obukhov Similarity Theory (MOST). The exact procedures to calculate r_x, r_s, and r_a are described in detail by Norman *et al.* (1995).

The canopy latent heat flux is derived using as an initial assumption a potential canopy transpiration, following the Priestley–Taylor equation:

$$LE_c = \alpha_{PT} f_g \left[\Delta / (\Delta + \gamma)\right] Rn_c \,, \tag{18}$$

where α_{PT} is the Priestley–Taylor coefficient (usually taken as 1.26), f_g is the green vegetation fraction, and Δ is the slope of the saturation vapor pressure *versus* temperature. If the vegetation is stressed, the Priestley–Taylor approximation overestimates the transpiration of the canopy and negative values of LE_S are computed. This improbable condensation over the soil during the daytime indicates the existence of vegetation water stress and it is solved by iteratively reducing α_{PT} and assuming LE_S equal to zero.

3. STUDY SITE

The study area is the agricultural area of Barrax in the centre of Spain (39°3′N, 2°6′W, 700 m a.s.l.) characterized by an alternation of irrigated and dry cultivated area, containing crops such as corn, barley, sunflower, alfalfa, and onions (Fig. 1). The climate is typically Mediterranean with vernal and autumnal rainfall, with an annual average of 400 mm, making it one of the driest areas in Europe.

Between 16 to 28 July 2012, the Regional Experiments For Land-atmosphere Exchanges (REFLEX) 2012 campaign has been carried out, where remote sensing and ground measurements used in this study have been collected (Timmermans *et al.* 2014). Hyper-spectral and thermal

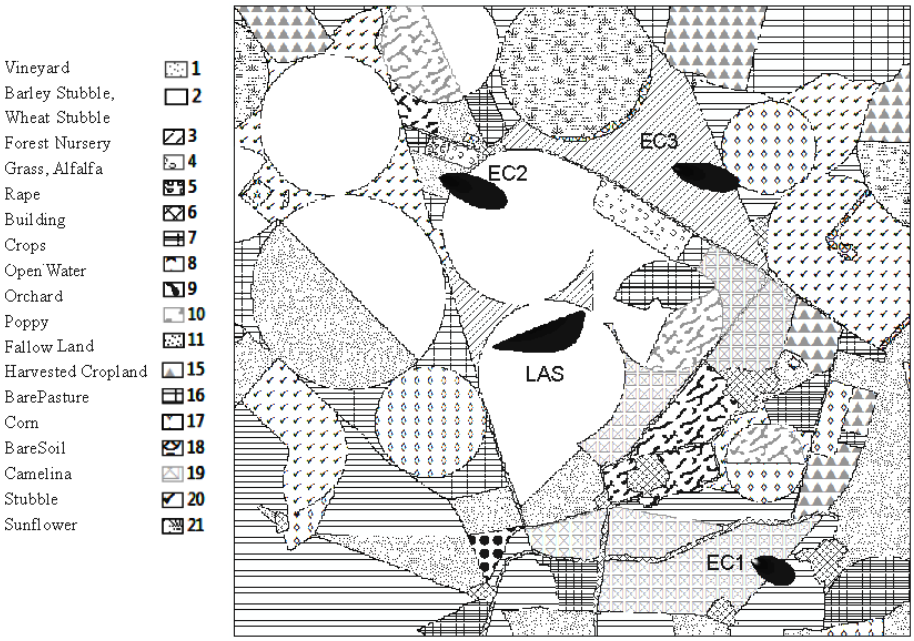

Fig. 1. Barrax agricultural area, land use, and footprint functions for 25 July at 9:28 UTC.

airborne images have been acquired during two days where for the entire period three eddy covariance towers and a large aperture scintillometer (LAS) have been installed. In selected points also some biophysical measurements have been carried out over different land-cover units comprising of Fractional Vegetation Cover (FVC), Leaf Area Index (LAI), Photosynthetically Active Radiation (PAR), and soil moisture (SM).

During the campaign, a large part of the crops were already harvested with the exception of maize, vineyard, sunflower, orchards, and forest nursery (see Fig. 1).

3.1 Ground data

Three micrometeorological towers and LAS sampled water and energy fluxes during the field campaign over different crop types. The first station (EC1) was located in a camelina field, the second one (EC2) in a small vineyard, and the third (EC3) in a forest nursery. The LAS was installed in a wheat-stubble field (van der Tol *et al.* 2015). Latent, sensible and soil heat fluxes were sampled in all fields, whereas net radiation was only recorded in EC1 and EC2. Station EC3 was also equipped with an infrared thermometer for determining outgoing longwave radiation. All meteorological data re-

quired by the models (incoming solar radiation, air temperature, air humidity, wind speed) were acquired by the stations. Soil moisture and soil temperature observations, which are needed also for post-processing the soil heat fluxes (van der Tol 2012), were obtained at the camelina site (EC1) as well.

Raw data from the EC towers have been corrected following the procedures well assessed in literature (Foken 2008). The EC1 and EC2 data have been analyzed with the Alteddy software (Alterra, WUR, Netherlands, http://www.climatexchange.nl/projects/alteddy/) whereas the EC3 data with the PEC software (Corbari *et al.* 2012) due to the availability of only thirty minutes average data. Corbari *et al.* (2014) compared corrected fluxes from high frequency and from 30 min average data in a maize field showing that low errors can be obtained with mean absolute daily difference equal to 6.1 $W\,m^{-2}$ for H and 13.2 $W\,m^{-2}$ for LE. The obtained fluxes observed by the four stations at the airborne overpass times are reported in Table 2. As well-known from the literature, there is a general lack of energy balance closure in EC measurements (Foken 2008, Twine *et al.* 2000, Wilson *et al.* 2002) although a reasonable small closure gap is obtained for EC1 and EC3. A poor behavior is obtained for EC2 in the vineyard field. This seems to be linked to the net radiation which, especially during daytime, becomes consistently higher than the sum of the other components of the energy balance equation. This is due to the fact that the field of view of the net radiometer is dominated by canopy, resulting in a lower albedo and thus higher net radiation then when seen from the altitude of the airborne sensors. The ratio G_0/Rn is quite high over these fields, in the range of 46 to 60% in respect to literature values (Su 2002, Choudhury *et al.* 1987). This might have been caused by very low winds, which indeed are occurring near the surface, especially over these fields. This is also noted in Su *et al.* (2008), who report

Table 2

Observed fluxes by the four stations and energy balance closure at 25 July at 9:28 UTC

Land use	Rn [W m^{-2}]	G_0 [W m^{-2}]	H [W m^{-2}]	LE [W m^{-2}]	$R_n - G_0$ [W m^{-2}]	$H + LE$ [W m^{-2}]	Energy budget closure [W m^{-2}]
Vineyard (EC2)	460	77	145	53	383	198	185
Camelina (EC1)	348	159	232	19	189	250	–62
Reforestation (EC3)	351	212	145	26	139	172	–33
Wheat stubble (LAS)	361	216	125				

similar rates for soil heat fluxes in the corridors between the vine stands in the same area in the same season, which were even not yet corrected for storage in the upper soil layer. Soil heat flux has also been shown to be a significant component in sparse vegetation (Kustas *et al.* 2000), and in semi-arid or arid regions G was found to account for up to 40% of Rn, which could be equal to or higher than LE (Verhoef *et al.* 1996).

The soil heat flux measurements at the individual sites were taken at depths of a few centimeters and needed to be corrected for storage in the soil layer above the sensors. Over the vineyard, one measurement was taken below the vine stand and another one in between the stands, so as to obtain representative observations for this particular site. Soil moisture and soil temperature observations were taken at different depths for the post-processing of the soil heat fluxes following the methodology described in van der Tol (2012). Unfortunately, these additional measurements were not taken at all four sites. However, following de Vries (1963) the soil heat flux may be described by:

$$G(z,t) = A(0)\,\mathrm{e}^{-z/D}\sqrt{\omega\rho c\lambda}\,\sin\left[\omega t - \frac{z}{D} + \frac{\pi}{4}\right], \tag{19}$$

where z [m] is the depth from the surface, t is time (unit the same as ω), $A(0)$ is the amplitude of the temperature wave at the surface [K], ω is the period of the soil heat flux (here taken as one day, unit taken in hours), ρ is the soil density [kg m^{-3}], c the soil specific heat [kJ kg^{-1} K^{-1}], λ the soil thermal conductivity [W m^{-1} K^{-1}], and D the so-called damping depth [m]. The corrections made at the camelina site were used in combination with Eq. 13 to derive D and the time delay of the temperature wave between 2 different depths. Assuming that soil properties in the area were homogeneous, these were then used to correct soil heat flux measurements taken at the other sites. A detailed discussion of the turbulent flux observations is provided in van der Tol *et al.* (2015), which includes a discussion of the well-known closure problem.

Large aperture scintillometers provide a measurement of the structure parameter for the refractive index, C_N^2 [m$^{-2/3}$], derived from the intensity fluctuations of an optical beam between a transmitter and a receiver. The structure parameter for the refractive index can be linked to the structure parameter for temperature, C_T^2 [K^2 m$^{-2/3}$], which, in turn, through the use of MOST and the temperature scale, T [K], can be used to derive the sensible heat flux, H. The physical background of measurements of this type is provided in Chehbouni *et al*. (2000), Lagouarde *et al.* (2002), Wang *et al.* (1978), whereas the method described in Timmermans *et al.* (2009) is used to extract the proper footprint area of the LAS observation.

The so-called source, or footprint, area of the LAS and EC towers are then computed to compare simulated and observed turbulent fluxes. The footprint of the eddy covariance towers and LAS originated from a south eastern wind. Details of all the micro-meteorological observations are provided in (van der Tol *et al.* 2015).

However, in most of the cases the intensity of the wind was not enough to cause contribution of other land use covers to the energy fluxes measurements. In the vineyard, however, the observation was influenced by the dry wheat-stubble during the time of plane overpass. For the validation of the modelled energy fluxes, a weighted integration of the pixels inside the footprint is computed in order to compare these values with the ground measurements (Timmermans *et al.* 2009). In Fig. 1 the spatial extent of the footprint areas for the analyzed moment of airplane overpass is shown.

3.2 Airborne data

During the campaign, 2 daytime and 1 nighttime flights of the CASA 212-200 N/S 270 "Paternina" airplane of INTA have been performed with the Airborne Hyperspectral Scanner (AHS) and Compact Airborne Imaging Spectrometer (CASI) sensors on board. The AHS sensor covers the thermal infrared part of the electromagnetic spectrum which is fundamental for estimating energy fluxes. A total of 13 daytime and 5 nighttime images are available at a spatial resolution of 4 m (Table 3). More details on these observations are provided in (de Miguel *et al.* 2015).

Table 3

FEST-EWB calibration against LST images from AHS

	Not calibrated				Calibrated			
UTC time	MAE [%]	MD (AHS-FEST-EWB) [°C]	MAD [°C]	RMSD [°C]	MAE [%]	MD (AHS-FEST-EWB) [°C]	MAD [°C]	RMSD [°C]
25 at 8:43	8.5	-0.6	3.0	4.1	4.8	–2.2	1.7	1.4
25 at 8:51	9.5	0.2	3.3	4.7	4.1	–1.9	1.7	1.8
25 at 9:02	8.9	1.3	3.4	5.1	3.7	0.7	1.9	2.9
25 at 9:11	9.5	2.5	3.1	4.4	3.5	0.9	1.9	2.7
25 at 9:19	8.6	1.7	2.9	4.3	3.9	–0.03	1.8	2.7
25 at 9:28	8.5	1.2	2.9	4.3	4.2	–0.7	1.0	1.8
25 at 9:38	8.3	0.9	3.1	4.4	3.1	–1.4	0.5	1.5
25 at 9:46	8.4	1.3	3.2	4.4	3.7	–1.1	1.4	2.2
26 at 8:42	11.1	–2.9	4.1	4.7	3.5	–2.9	1.2	1.8
26 at 8:51	12.1	2.7	3.8	4.8	2.4	1.8	1.5	2.2
26 at 9:07	10.3	2.8	3.3	4.3	3.0	0.15	1.8	2.5
26 at 9:25	7.8	1.3	2.7	3.9	3.2	0.21	0.9	1.7
26 at 9:38	11.9	–3.2	5.1	6.2	1.2	–5.4	2.4	2.3
All images	9.5	0.7	3.4	4.6	3.4	–0.9	1.5	2.1

Land surface temperature values are obtained with the Temperature and Emissivity Separation method (TES) described in Gillespie *et al.* (1998) and applied to AHS data following Sobrino *et al.* (2008). The entire dataset was used for FEST-EWB model calibration, whereas the TSEB and FEST-EWB validation is performed for the image acquired on 25 July at 9:28 UTC.

Additional remote sensing based input, required, such as albedo, NDVI, LAI, and f_v was computed following Timmermans *et al*. (2011) and Richter and Timmermans (2009).

4. RESULTS

The results focus on the comparison between model output of FEST-EWB and TSEB for 25 July at 9:28 UTC. Simulated energy fluxes for both models are validated *versus* ground observations of these fluxes over different land-cover types. Use is made of the data collected in the 4 aforementioned observation sites. Furthermore, a spatial intercomparison of the two models is made, in order to investigate also model output not covered by any one of the four validation sites.

For the evaluation of the models, different statistics are utilized: the mean difference (MD), the mean absolute difference (MAD), the mean absolute error (MAE), the root mean square difference (RMSD), the mean value (MA), and its standard deviation (SD):

$$\mathrm{MA} = \frac{\sum_{i=1}^{n}\left(X_i\right)}{n}\ , \tag{20}$$

$$\mathrm{SD} = \left[\frac{\sum_{i=1}^{n}\left(X_i - \mathrm{MA}\right)^2}{n-1}\right]^{0.5}\ , \tag{21}$$

$$\mathrm{MD} = \frac{\sum_{i=1}^{n}\left(X_i - Y_i\right)}{n}\ , \tag{22}$$

$$\mathrm{MAD} = \frac{\sum_{i=1}^{n}\left|X_i - Y_i\right|}{n}\ , \tag{23}$$

$$\mathrm{MAE} = \frac{100}{\mathrm{MA}}\left(\frac{\sum_{i=1}^{n}\left|X_i - Y_i\right|}{n}\right)\ , \tag{24}$$

$$\mathrm{RMSD} = \left[\frac{\sum_{i=1}^{n} \left(X_i - Y_i \right)^2}{n} \right]^{0.5}, \tag{25}$$

where X_i and Y_i are the ith observed or measured variable, and n is the sample size.

4.1 Models calibration

4.1.1 FEST-EWB calibration

FEST-EWB is run in a continuous mode at a temporal resolution of 10 min and at the spatial resolution of 4 m. The configuration is simplified without computing surface and subsurface discharges and without snow dynamics which are considered not relevant for the area of interest.

The initial conditions of the model are derived from distributed soil moisture measurements made during the field campaign in the different fields. The simulation time is from 24 to 26 July, as such using the entire dataset of AHS images.

The calibration procedure is based on a pixel-to-pixel modification of the soil and vegetation parameters (Table 1) used as input in the model through the minimization of the differences between the model internal state variable RET and the remotely observed LST. This innovative methodology is based on remote sensing images of land surface temperature and provides the opportunity to calibrate and validate the distributed hydrological model in each pixel of the domain when ground data of evapotranspiration or discharge are not available. Moreover, with this methodology there is a possibility to calibrate model's internal state variables (*e.g.*, land surface temperature) in addition to the traditional external fluxes (*e.g.*, discharge) to obtain better understanding of hydrologic process and model analysis at pixel scale (Dooge 1986). In fact, a traditional calibration (as typically done in classical hydrological models) is based only on ground discharge data in few rivers sections. Such an approach lumps all the hydrological processes together so that the correct spatial determination of mass and energy fluxes is more difficult. Instead, when a pixel by pixel calibration is performed, a better spatial distribution should be achieved. Corbari and Mancini (2013) and Corbari *et al.* (2015) demonstrated the reliability of this procedure for two different case studies in Italy and China.

Soil parameters have been defined starting from the soil type of the area taken from the Harmonized World Soil Database (FAO/IIASA/ISRIC/ISSCAS/JRC 2009). The parameter values are modified paying attention that their values remain within their physical ranges (Rawls and Brakensiek 1985).

In Table 3 the difference statistics between LST from AHS and RET for the different available flights are shown. FEST-EWB before calibration generally overestimates observed values, while after the calibration a reasonable agreement is reached with RMSD that goes from 4.6 to 2.1 °C.

4.1.2 TSEB calibration

The TSEB model does not require any calibration, since it is entirely physically based. A minor exception is made in the current contribution, however. The constant used in Eq. 14 that describes the ratio between soil heat flux and net radiation reaching the soil is calibrated using local observations. For the time of overpass, the adjusted coefficient, c_g, equals 0.48 (-) instead of the original value of 0.35 (-) (Andreu *et al.* 2015). This higher value reflects the arid conditions in the area under study, where typically a large part of the radiation is used for heating up the soil surface. The effect of the calibration of this c_g factor has an average increasing effect of 33 $\mathrm{Wm^{-2}}$ on G_0 (28 $\mathrm{Wm^{-2}}$ for forest nursery, 36 $\mathrm{Wm^{-2}}$ for wheat, 30 $\mathrm{Wm^{-2}}$ for camelina, and 38 $\mathrm{Wm^{-2}}$ for vineyard) and a similar decreasing effect, mainly on H (due to the fact that LE is generally low in the area).

4.2 Models intercomparison

4.2.1 Point validation

The comparison between modelled energy fluxes by both models with measured values yields a general good agreement, as shown in Fig. 2. Statistical comparison between modelled and measured fluxes is then shown in Table 4 in terms of MAD and MAE.

Table 4

Statistics between energy fluxes modelled by the FEST-EWB and TSEB models with measured values for 25 July at 9:28 UTC

		EC1		EC2		EC3		LAS	
		MAD [$\mathrm{Wm^{-2}}$]	MAE [%]	MAD [$\mathrm{Wm^{-2}}$]	MAE [%]	MAD [$\mathrm{Wm^{-2}}$]	MAE [%]	MAD [$\mathrm{Wm^{-2}}$]	MAE [%]
Rn	FEST-EWB	22	6	140	30	10	3	56	15
Rn	TSEB	29	8	140	30	26	7	67	19
G	FEST-EWB	51	32	10	13	98	46	146	68
G	TSEB	49	31	62	81	110	52	82	38
H	FEST-EWB	40	17	60	41	33	23	11	9
H	TSEB	41	18	4	3	38	26	8	6
LE	FEST-EWB	7	38	7	12	12	47		
LE	TSEB	1	5	13	25	13	49		

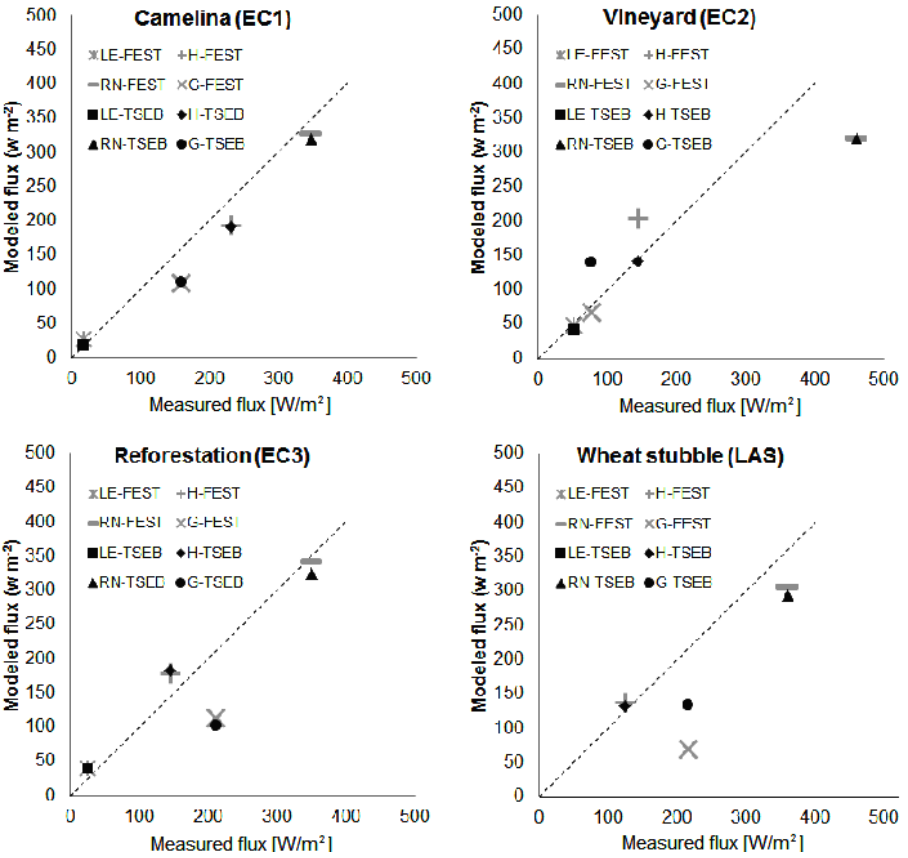

Fig. 2. Comparison between energy fluxes modelled by the FEST-EWB and TSEB models with measured values for 25 July at 9:28 UTC.

In general, according to Fig. 2 a good agreement is found between all observed and modelled energy fluxes in EC1. The EC3 results are still in a reasonable agreement with observations, except for *G*. Instead, a larger residual is found in Vineyard EC2 site (~185 Wm^{-2}), probably related to net radiometer positioning, but also due to turbulent source area which sometimes is bigger than the vineyard field.

The observed and modelled net radiation estimates are in a similar agreement for both models with MAD between 10 and 67 Wm^{-2}, except for the vineyard stations where MAD reaches 140 Wm^{-2}. This is attributed to the net radiometer positioning, as mentioned above.

Soil heat fluxes present large discrepancies between observed and modelled values by both models, in particular in the reforestation and in the wheat stubble fields with MAD reaching values of 146 Wm^{-2}. However,

observations of *G* are very local and can vary a lot over just few meters, especially over sparsely and heterogeneously vegetated areas (Kustas *et al.* 2000). In the light of this high spatial variation of soil heat flux, the number of soil heat flux observations was rather limited. Most probably, they were insufficient to cover the full range of spatial variation at several observation sites. This holds especially true for the soil heat flux observations made at the wheat stubble field and the reforestation area. Typically at these sites the soil heat flux plates had to be buried at locations characterized by a low canopy cover. As such, the observations made at these sites are most probably higher than the representative site average.

Turbulent fluxes are generally well reproduced by both models. The modelled values are weighted according to the stations footprint estimates in order to be comparable to measured fluxes (as described in Section 3.1).

The MAD for sensible heat flux in the four stations from FEST-EWB is between some 10 and 60 Wm^{-2}, while for TSEB it is between 5 and 40 Wm^{-2}. Good agreements are obtained for the latent heat flux showing even lower MAD values, under 15 Wm^{-2}, for both models in the three eddy covariance sites, comparable with the measurement uncertainties. Anyhow, it should be noted that the measured LE values are generally very low, between some 20 and 50 Wm^{-2}, meaning that only small range of model applicability is tested.

It is interesting to note the large differences in the *H* performances between the two models over the vineyard, where TSEB reaches MAD values of 4 Wm^{-2} and MAE of 3%, while FEST-EWB shows values of 60 Wm^{-2} and 41%, respectively. This discrepancy is attributed to the different nature of the models. TSEB is a two-source model which works better for high and partially vegetated area, such as is the case in the vineyard field. FEST-EWB is based on an equilibrium temperature and, despite FEST-EWB differentiates between soil and vegetation resistances, a single representative equilibrium temperature is computed.

This result over the vineyard confirms previous findings by Kustas and Norman (1999), Timmermans *et al.* (2007), Crow *et al.* (2005), although the sparsely vegetated forest nursery shows similar results for both models. However, the vegetation cover is so low over this site that the vegetation contribution to the fluxes is almost negligible.

Nevertheless, with the notable exception of part of the deviating *Rn* and *G* observations, the overall model performances are rather good. RMSD values are comparable or better than those obtained in previous validation studies (French *et al.* 2005, Kustas *et al.* 2012, Timmermans *et al.* 2007, Cammalleri *et al.* 2012).

4.2.2 Distributed validation

To understand the reliability and variability of the two models estimates, spatially distributed analyses are performed, which are even more important in extremely heterogeneous area such as Barrax site where high differences in magnitude of latent and sensible heat fluxes are present. Despite the good agreement at the flux towers, which are typically positioned at larger fields comprising of a uniform cover, spatial intercomparison of the FEST-EWB and TSEB models (Fig. 3) reveals significant discrepancies. An exception is made for the net radiation estimates, which show a rather similar behavior for both models (see Fig. 3 and Table 5).

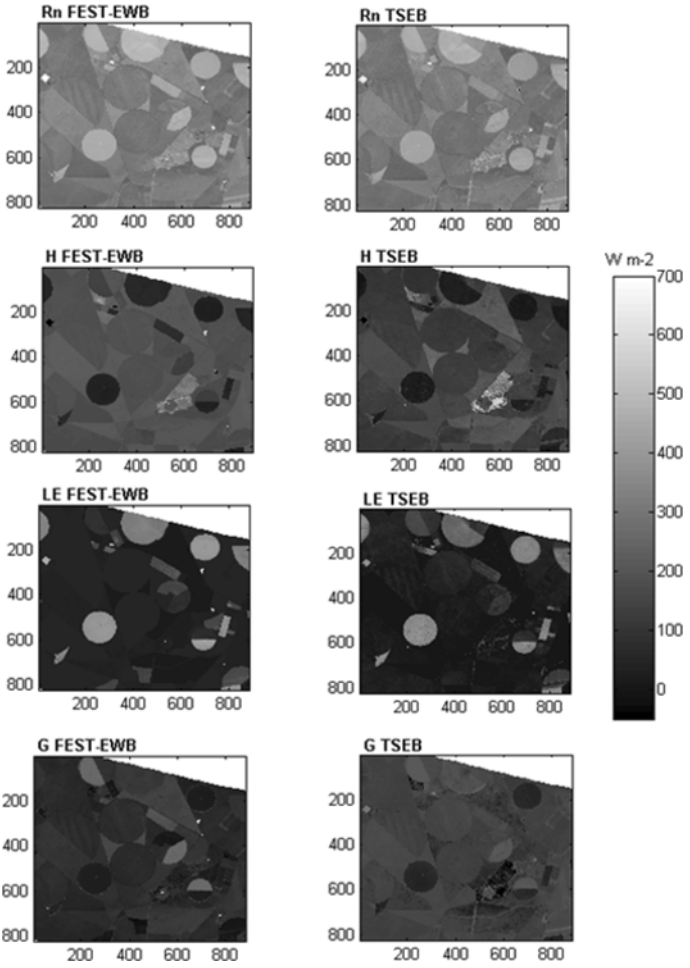

Fig. 3. Spatial MD values of the energy fluxes between TSEB minus FEST-EWB for 25 July at 9:28 UTC.

Table 5

Spatial statistics between energy fluxes modelled by the FEST-EWB and TSEB models for 25 July at 9:28 UTC

	MA (TSEB) [W m^{-2}]	SD (TSEB) [W m^{-2}]	MA (FEST-EWB) [W m^{-2}]	SD (FEST-EWB) [W m^{-2}]	AE [%]	MD (TSEB-FEST-EWB) [W m^{-2}]	MAD [W m^{-2}]	RMSD [W m^{-2}]
Rn	330	58.1	339	64	5.2	–8.7	18.4	23
G	136	47	82	44	145.9	54.2	68.1	60
H	135	67	177	54	31.7	–36.3	51.5	40
LE	59	95	80	100	60.9	–15.9	32.1	38

Relative to FEST-EWB model, TSEB yields smaller (larger) average estimates of *LE* and *H* (*G*) while predicting a similar spatial variation in all fluxes (Table 5). These results are also supported by the frequency diagrams of each flux from the two models (Fig. 4) which highlight a significant heterogeneity in the fluxes due to the high thermodynamic heterogeneity of the Barrax area.

These plots show that *Rn* from FEST-EWB and TSEB have the same shape as well as the same mean and standard deviation values, while for *G* the mean for TSEB is some 50 Wm^{-2} lower than for FEST-EWB despite having a similar standard deviation. The turbulent fluxes histograms have a quasi-bimodal distribution for both models due to the distinction between irrigated crops and bare soil or harvest crops. Moreover, the latent heat flux histogram shows a higher tail-end, ranging from 300 to 700 W m^{-2}. These are due to the presence of small fields with crops at different growth stages and with different soil moisture conditions.

Spatial variability in flux predictions is driven largely by differences in landcover types with different vegetation fraction and different irrigation practice. To demonstrate how these two fundamentally different models treat these different landcover types and different spatial variation, different statistics are computed for each landcover (Fig. 5).

These analyses confirm the agreement between the two models for net radiation with absolute mean difference less than 30 Wm^{-2}, but also the generally high discrepancies in soil heat flux estimates. As also commented in Section 4.2.1, *G* is a difficult variable to assess its reliability; moreover, the models have a very different algorithm for its computation. TSEB computed and calibrated *G* using the ratio with *Rn* reaching the soil (Eq. 14), while the *G* estimation in FEST-EWB is based on the heat conduction equation (Eq. 7).

For almost all landcover types, with the main exception of the well-irrigated grassland, TSEB shows larger values for *G*. This may be attributed

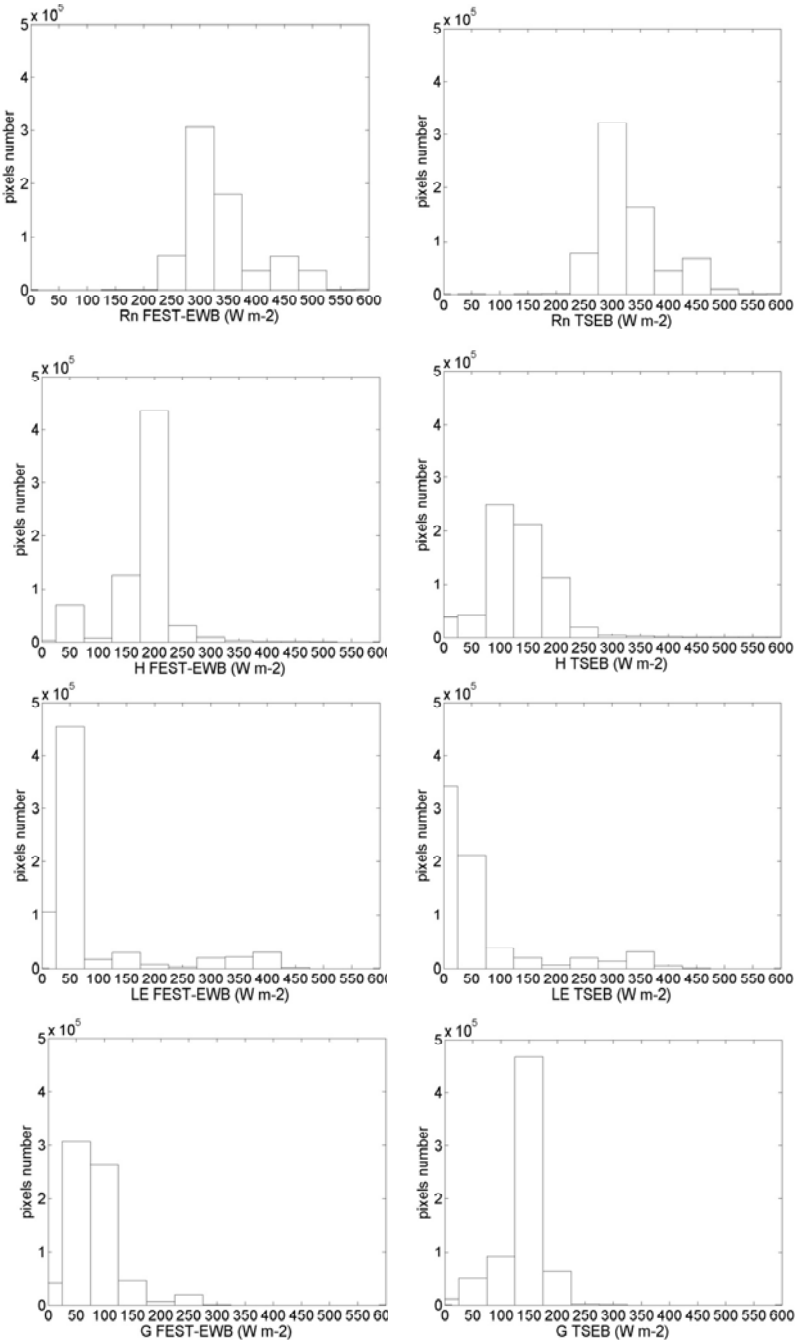

Fig. 4. Histograms of the energy fluxes of TSEB and FEST-EWB for 25 July at 9:28 UTC.

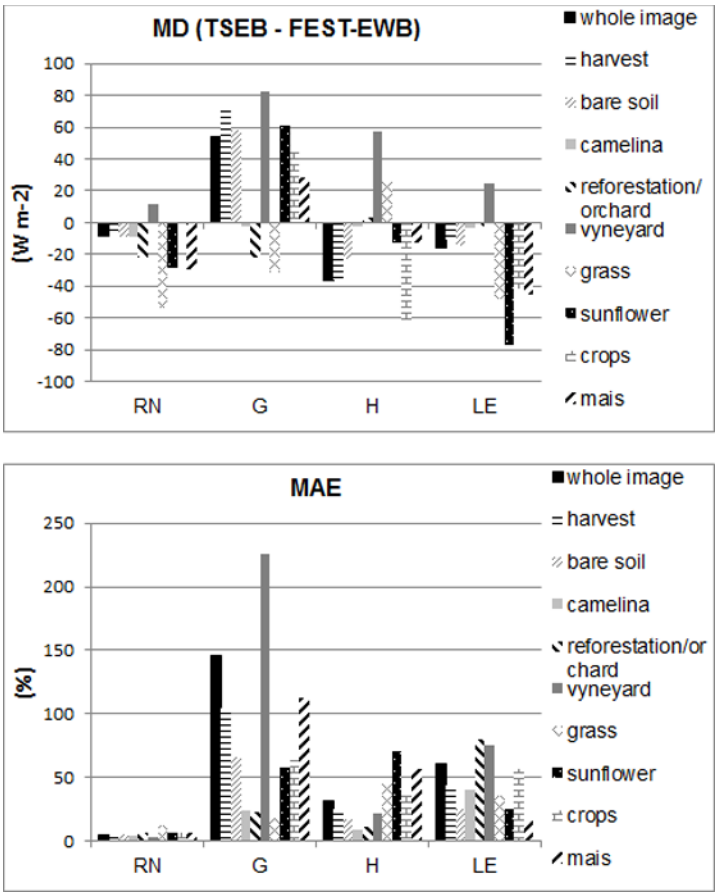

Fig. 5. Spatial statistics between energy fluxes modelled by the FEST-EWB and TSEB models for 25 July at 9:28 UTC divided by landcover classes.

to the local calibration performed in TSEB with respect to G estimates. The value of c_g in Eq. 14 was increased by some 40% with respect to the original formulation of TSEB due to this calibration. At average values of G between 130 and 140 $\mathrm{W\,m^{-2}}$ this explains a large part of the observed difference with FEST-EWB.

The turbulent fluxes behavior is discordant between the different land-covers. The bare soil, camelina, stubble, and harvest fields are characterized by a uniform coverage and extremely high land surface temperature, and a reasonable agreement between the two models in terms of H and also of LE is reached. In the reforestation field a general agreement on all fluxes is noted.

Relatively high differences in latent and sensible heat fluxes between the models are noted in the vineyard field, as can be explained from the dual source character of TSEB. FEST-EWB provides lower estimates of G and LE and especially of H with respect to TSEB (Fig. 5) in this landcover type. This is also the reason why TSEB shows higher values for H over the orchard, which is a landcover type that is typically represented better by a two-source approach.

The grass, sunflower, crops and maize fields are irrigated crops with low land surface temperature values which cause high evapotranspiration fluxes. Relatively high MAD values, between 38 and 80 Wm^{-2}, are obtained for G, LE and H, where FEST-EWB shows higher estimates of latent and sensible heat fluxes than TSEB which in turn shows higher values for the ground heat flux.

A rather striking difference is seen in recently irrigated fields that are irrigated by rotating pivot systems. Recently irrigated land, for example noted in the large sunflower field in the north of the area, shows a drastically lower LST resulting in a lower H for TSEB as compared to that part of the field that is not yet irrigated. Since LST is not an input to FEST, this within-field difference does not appear in the FEST-EWB results. This indicates that the thermo-dynamic variation is reflected better in the TSEB approach.

Therefore, within-field variation of the evaporative fraction is noted more clearly in the TSEB output. The FEST-EWB model computes, in addition to the energy budget, also the water balance, for which the irrigation amount is an important input. As mentioned above, some fields are irrigated with a rotating pivot. For FEST-EWB this means that knowing its exact position during the airborne overpasses is almost a must.

5. DISCUSSION AND CONCLUSIONS

An intercomparison between the Energy Water Balance model (FEST-EWB) and Two-Source Energy Balance model (TSEB) has been performed over an extremely heterogeneous agricultural area with respect crop fraction and soil moisture conditions.

Both models performed well against energy fluxes measured at the eddy covariance stations and at the large aperture scintillometer. However, when a spatial analysis is performed, significant differences between the two approaches are highlighted, showing an agreement between the two for net radiation with absolute mean difference less than 30 Wm^{-2}, but also high discrepancies in soil heat flux estimates. Latent and sensible heat fluxes have discordant behavior for the different landcovers with reasonable agreement over uniform coverage area while high differences over sparse landcover and irrigated fields. In general, model outputs were comparable over large and

homogeneous fields whereas discrepancies were mainly noted over relatively small and sparsely vegetated heterogeneous areas.

Models, like TSEB, that use LST from remote sensing as an input parameter may provide generally accurate instantaneous estimates in particular of *H*, although a certain sensitivity related to LST accuracy should be considered. Instead, hydrological models, like FEST-EWB, provide continuous estimates of soil moisture dynamic and energy fluxes overcoming the limitations related to temporal integration, typical of flux estimates based solely on remote sensing input, and cloud coverage, typical of satellite images. Therefore, they are usually more complex and over-parameterized so that a precise calibration is always needed in contrast to a model using remote sensing input only. Another disadvantage is the need of the timing and volume of irrigation that are not always easy to obtain.

Despite the completely different approaches of the two models, a rather well spatial agreement is noted for most of the landcover types, especially over larger fields with a uniform vegetation cover. Small-scale variations in turbulent flux exchange are better reflected in the remote sensing-based TSEB model. This highlights the idea that instantaneous sensible heat flux estimates of TSEB could be assimilated to update the state of a continuous distributed hydrological model in order to obtain a robust tool for water resources management.

Acknowledgments. The research leading to these results has received funding from the European Community's 7th Framework Programme (FP7/2008-2013) under EUFAR contract No. 227159, Cost Action ES0903-EUROSPEC, and ESA Grant D/EOP/rp/2012/48. We would like to thank Christiaan van der Tol, Joris Timmermans, Murat Uçer, Xuelong Chen, Zhongbo Su, Marco Mancini, Giuseppe Milleo, Alessandro Ceppi, and Arnaud Carrara who helped with the measurements.

References

Anderson, M.C., J.M. Norman, W.P. Kustas, F. Li, J.H. Prueger, and J.R. Mecikalski (2005), Effects of vegetation clumping on two-source model estimates of surface energy fluxes from an agricultural landscape during SMACEX, *J. Hydrometeorol.* **6**, 6, 892-909, DOI: 10.1175/JHM465.1.

Andreu, A., W.J. Timmermans, D. Skokovic, and M.P. Gonzalez-Dugo (2015), Influence of component temperature derivation from dual angle thermal infrared observations on TSEB flux estimates over an irrigated vineyard, *Acta Geophys.* **63**, 6, 1540-1570, DOI: 10.1515/acgeo-2015-0037 (this issue).

Bastiaanssen, W.G.M., M. Menenti, R.A. Feddes, and A.A.M. Holtslag (1998), A remote sensing surface energy balance algorithm for land (SEBAL). 1. Formulation, *J. Hydrol.* **212-213**, 198-212, DOI: 10.1016/S0022-1694(98)00253-4.

Brath, A., A. Montanari, and E. Toth (2004), Analysis of the effects of different scenarios of historical data availability on the calibration of a spatially-distributed hydrological model, *J. Hydrol.* **291**, 3-4, 232-253, DOI: 10.1016/j.jhydrol.2003.12.044.

Brutsaert, W. (1982), *Evaporation into the Atmosphere*, Reidel, Dordrecht.

Brutsaert, W. (2005), *Hydrology: An Introduction*, Cambridge University Press, Cambridge.

Cammalleri, C., M.C. Anderson, G. Ciraolo, G. D'Urso, W.P. Kustas, G. La Loggia, and M. Minacapilli (2012), Applications of a remote sensing-based two-source energy balance algorithm for mapping surface fluxes without in situ air temperature observations, *Remote Sens. Environ.* **124**, 502-515, DOI: 10.1016/j.rse.2012.06.009.

Chehbouni, A., C. Watts, J.-P. Lagouarde, Y.H. Kerr, J.-C. Rodriguez, J.-M. Bonnefond, F. Santiago, G. Dedieu, D.C. Goodrich, and C. Unkrich (2000), Estimation of heat and momentum fluxes over complex terrain using a large aperture scintillometer, *Agr. Forest Meteorol.* **105**, 1-3, 215-226, DOI: 10.1016/S0168-1923(00)00187-8.

Chehbouni, A., J.C.B. Hoedjes, J.-C. Rodriguez, C.J. Watts, J. Garatuza, F. Jacob, and Y.H. Kerr (2008), Using remotely sensed data to estimate area-averaged daily surface fluxes over a semi-arid mixed agricultural land, *Agr. Forest Meteorol.* **148**, 330-342, DOI: 10.1016/j.agrformet.2007.09.014.

Choudhury, B.J., S.B. Idso, and R.J. Reginato (1987), Analysis of an empirical model for soil heat flux under a growing wheat crop for estimating evaporation by an infrared-temperature based energy balance equation, *Agr. Forest Meteorol.* **39**, 4, 283-297, DOI: 10.1016/0168-1923(87)90021-9.

Corbari, C., and M. Mancini (2013), Calibration and validation of a distributed energy – water balance model using satellite data of land surface temperature and ground discharge measurements, *J. Hydrometeorol.* **15**, 1, 376-392, DOI: 10.1175/JHM-D-12-0173.1.

Corbari, C., G. Ravazzani, J. Martinelli, and M. Mancini (2009), Elevation based correction of snow coverage retrieved from satellite images to improve model calibration, *Hydrol. Earth Syst. Sci.* **13**, 639-649, DOI: 10.5194/hess-13-639-2009.

Corbari, C., J.A. Sobrino, M. Mancini, and V. Hidalgo (2010), Land surface temperature representativeness in a heterogeneous area through a distributed energy-water balance model and remote sensing data, *Hydrol. Earth Syst. Sci.* **14**, 2141-2151, DOI: 10.5194/hessd-7-5335-2010.

Corbari, C., G. Ravazzani, and M. Mancini (2011), A distributed thermodynamic model for energy and mass balance computation: FEST-EWB, *Hydrol. Process.* **25**, 9, 1443-1452, DOI: 10.1002/hyp.7910.

Corbari, C., D. Masseroni, and M. Mancini (2012), Effetto delle correzioni dei dati misurati da stazioni eddy covariance sulla stima dei flussi evapotraspirativi, *Ital. J. Agrometeorol.* **1**, 35-51 (in Italian).

Corbari, C., J.A. Sobrino, M. Mancini, and V. Hidalgo (2013), Mass and energy flux estimates at different spatial resolutions in a heterogeneous area through a distributed energy-water balance model and remote-sensing data, *Int. J. Remote Sens.* **34**, 9-10, 3208-3230, DOI: 10.1080/ 01431161. 2012.716924.

Corbari C., D. Masseroni, A. Ceppi, A. Facchi, C. Gandolfi, and M. Mancini (2014), Comparison between high frequency and thirty minutes averaged data from eddy covariance measurements for operative water management, *J. Irrig. Drainage Eng*. (in review).

Corbari, C., M. Mancini, J. Li, and Z. Su (2015), Can satellite land surface temperature data be used similarly to river discharge measurements for distributed hydrological model calibration?, *Hydrol. Sci. J.* **60**, 2, 202-217, DOI: 10.1080/02626667.2013.866709.

Crow, W.T., E.F. Wood, and M. Pan (2003), Multiobjective calibration of land surface model evapotranspiration predictions using streamflow observations and spaceborne surface radiometric temperature retrievals, *J. Geophys. Res.* **108**, D23, 4725, DOI: 10.1029/2002JD003292.

Crow, W.T., F. Li, and W.P. Kustas (2005), Intercomparison of spatially distributed models for predicting surface energy flux patterns during SMACEX, *J. Hydrometeorol.* **6**, 6, 941-953, DOI: 10.1175/JHM468.1.

Crow, W.T., W.P. Kustas, and J.H. Prueger (2008), Monitoring root zone soil moisture though the assimilation of a thermal remote sensing-based soil moisture proxy into a water balance model, *Remote Sens. Environ.* **112**, 4, 1268-1281, DOI: 10.1016/j.rse.2006.11.033.

Dai, Y., X. Zeng, R.E. Dickinson, I. Baker, G.B. Bonan, M.G. Bosilovich, A. Scott Denning, P.A. Dirmeyer, P.R. Houser, G. Niu, K.W. Oleson, C. Adam Schlosser, and Z.-L. Yang (2003), The Common Land Model, *Bull. Amer. Meteor. Soc.* **84**, 8, 1013-1023, DOI: 10.1175/BAMS-84-8-1013.

de Miguel, E., M. Jiménez, I. Pérez, Ó.G. de la Cámara, F. Muñoz, and J.A. Gómez-Sánchez (2015), AHS and CASI processing for the REFLEX remote sensing campaign: methods and results, *Acta Geophys.* **63**, 6, 1485-1498, DOI: 10.1515/ acgeo-2015-0031 (this issue).

de Vries, D.A. (1963), Thermal properties of soils. **In:** W.R. van Wijk (ed.), *Physics of Plant Environment*, North Holland, Amsterdam, 210-233.

Dooge, J.C.I. (1986), Looking for hydrologic laws, *Water Resour. Res.* **22**, 9S, 46-58, DOI: 10.1029/WR022i09Sp0046S.

Famiglietti, J.S., and E.F. Wood (1994), Multiscale modeling of spatially variable water and energy balance processes, *Water Resour. Res.* **30**, 11, 3061-3078, DOI: 10.1029/94WR01498.

FAO/IIASA/ISRIC/ISSCAS/JRC (2009), Harmonized world soil database (version 1.1), FAO, Rome, Italy and IIASA, Laxenburg, Austria.

Foken, T. (2008), *Micrometeorology*, Springer, Berlin.

Franks, S.W., and K.J. Beven (1999), Conditioning a multiple-patch SVAT Model using uncertain time-space estimates of latent heat fluxes as inferred from remotely sensed data, *Water Resour. Res.* **35**, 9, 2751-2761, DOI: 10.1029/1999WR900108.

French, A.N., F. Jacob, M.C. Anderson, W.P. Kustas, W. Timmermans, A. Gieske, Z. Su, H. Su, M.F. McCabe, F. Li, J. Prueger, and N. Brunsell (2005), Surface energy fluxes with the Advanced Spaceborne Thermal Emission and Reflection radiometer (ASTER) at the Iowa 2002 SMACEX site (USA), *Remote Sens. Environ.* **99**, 1-2, 55-65, DOI: 10.1016/j.rse.2005.05.015.

Gillespie, A., S. Rokugawa, T. Matsunaga, J.S. Cothern, S. Hook, and A.B. Kahle (1998), A temperature and emissivity separation algorithm for Advanced Spaceborne Thermal Emission and Reflection Radiometer (ASTER) images, *IEEE Geosci. Remote S.* **36**, 4, 1113-1126, DOI: 10.1109/36.700995.

Gonzalez-Dugo, M.P., C.M.U. Neale, L. Mateos, W.P. Kustas, J.H. Prueger, M.C. Anderson, and F. Li (2009), A comparison of operational remote sensing-based models for estimating crop evapotranspiration, *Agr. Forest Meteorol.* **149**, 11, 1843-1853, DOI: 10.1016/j.agrformet.2009.06.012.

Gutmann, E.D., and E.E. Small (2010), A method for the determination of the hydraulic properties of soil from MODIS surface temperature for use in land-surface models, *Water Resour. Res.* **46**, 6, W06520, DOI: 10.1029/2009WR008203.

Huntingford, C., S.J. Allen, and R.J. Harding (1995), An intercomparison of single and dual-source vegetation-atmosphere transfer models applied to transpiration from sahelian savannah, *Bound.-Lay. Meteorol.* **74**, 4, 397-418, DOI: 10.1007/BF00712380.

Jarvis, P.G. (1976), The interpretation of the variations in leaf water potential and stomatal conductance found in canopies in the field, *Phil. Trans. R. Soc. Lond. B* **273**, 593-610, DOI: 10.1098/rstb.1976.0035.

Kustas,W.P., and J.M. Norman (1999), Evaluation of soil and vegetation heat flux predictions using a simple two-sourcemodel with radiometric temperatures for partial canopy cover, *Agr. Forest Meteorol.* **94**, 1, 13-29, DOI: 10.1016/S0168-1923(99)00005-2

Kustas, W.P., K.S. Humes, J.M. Norman, and M.S. Moran (1996), Single- and dual-source modeling of surface energy fluxes with radiometric surface temperature, *J. Appl. Meteor.* **35**, 1, 110-121, DOI: 10.1175/1520-0450(1996)035<0110:SADSMO>2.0.CO;2.

Kustas, W.P., X. Zhan, and T.J. Schmugge (1998), Combining optical and microwave remote sensing for mapping energy fluxes in a semiarid watershed, *Remote Sens. Environ.* **64**, 2, 116-131, DOI: 10.1016/S0034-4257(97)00176-4.

Kustas, W.P., J.H. Prueger, J.L. Hatfield, K. Ramalingam, and L. Hipps (2000), Variability in soil heat flux from a mesquite dune site, *Agr. Forest Meteorol.* **103**, 3, 249-264, DOI: 10.1016/S0168-1923(00)00131-3.

Kustas, W.P., M.C. Anderson, A.N. French, and D. Vickers (2006), Using a remote sensing field experiment to investigate flux-footprint relations and flux sampling distributions for tower and aircraft-based observations, *Adv. Water Resour.* **29**, 2, 355-368, DOI: 10.1016/j.advwatres.2005.05.003.

Kustas, W.P., J.G. Alfieri, M.C. Anderson, P.D. Colaizzi, J.H. Prueger, S.R. Evett, C.M.U. Neale, A.N. French, L.E. Hipps, J.L. Chávez, K.S. Copeland, and T.A. Howell (2012), Evaluating the two-source energy balance model using local thermal and surface flux observations in a strongly advective irrigated agricultural area, *Adv. Water Resour.* **50**, 120-133, DOI: 10.1016/j.advwatres.2012.07.005.

Lagouarde, J.-P., F. Jacob, X.F. Gu, A. Olioso, J.-M. Bonnefond, Y. Kerr, K.J. McAneney, and M. Irvine (2002), Spatialization of sensible heat flux over a heterogeneous landscape, *Agronomie* **22**, 6, 627-633, DOI: 10.1051/agro:2002032.

Lhomme, J.-P., and A. Chehbouni (1999), Comments on dual-source vegetation-atmosphere transfer models, *Agr. Forest Meteorol.* **94**, 3-4, 269-273, DOI: 10.1016/S0168-1923(98)00109-9.

Liang, X., D.P. Lettenmaier, E.F. Wood, and S.J. Burges (1994), A simple hydrologically based model of land surface water and energy fluxes for GCMs, *J. Geophys. Res.* **99**, D7, 14415-14428, DOI: 10.1029/94JD00483.

Mancini, M. (1990), La modellazione distribuita della risposta idrologica: effetti della variabilità spaziale e della scala di rappresentazione del fenomeno dell'assorbimento, Ph.D. Thesis, Politecnico di Milano, Milan (in Italian).

McCumber, M.C., and R.A. Pielke (1981) Simulation of the effects of surface fluxes of heat and moisture in a mesoscale numerical model: 1. Soil layer, *J. Geophys. Res.* **86**, C10, 9929-9938, DOI: 10.1029/JC086iC10p09929.

Norman, J.M., W.P. Kustas, and K.S. Humes (1995), Source approach for estimating soil and vegetation energy fluxes in observations of directional radiometric surface temperature, *Agr. Forest Meteorol.* **77**, 3-4, 263-293, DOI: 10.1016/0168-1923(95)02265-Y.

Rabuffetti, D., G. Ravazzani, C. Corbari, and M. Mancini (2008), Verification of operational Quantitative Discharge Forecast (QDF) for a regional warning system – the AMPHORE case studies in the upper Po River, *Nat. Hazards Earth Syst. Sci.* **8**, 161-173, DOI: 10.5194/nhess-8-161-2008.

Ravazzani, G., D. Rametta, and M. Mancini (2011), Macroscopic Cellular Automata for groundwater modelling: A first approach, *Environ. Modell. Softw.* **26**, 5, 634-643, DOI: 10.1016/j.envsoft.2010.11.011.

Rawls, W.J., and D.L. Brakensiek (1985), Prediction of soil water properties for hydrologic modeling. **In:** E.B. Jones and T.J. Ward (eds.), *Watershed Management in the Eighties*, *A Symposium of ASCE Convention; April 30-May 1, 1985, Denver, Colorado, United States,* ASCE, New York, NY, 293-299.

Richter, K., and W.J. Timmermans (2009), Physically based retrieval of crop characteristics for improved water use estimates, *Hydrol. Earth Syst. Sci.* **13**, 5, 663-674, DOI: 10.5194/hess-13-663-2009.

Roerink, G.J., Z. Su, and M. Menenti (2000), S-SEBI: A simple remote sensing algorithm to estimate the surface energy balance, *Phys. Chem. Earth B* **25**, 2, 147-157, DOI: 10.1016/S1464-1909(99)00128-8.

Sobrino, J.A., J.C. Jiménez-Muñoz, G. Sòria, M. Gómez, A. Barella Ortiz, M. Romaguera, M. Zaragoza, Y. Julien, J. Cuenca, M. Atitar, V. Hidalgo, B. Franch, C. Mattar, A. Ruescas, L. Morales, A. Gillespie, L. Balick, Z. Su, F. Nerry, L. Peres, and R. Libonati (2008), Thermal remote sensing in the framework of the SEN2FLEX project: field measurements, airborne data and applications, *Int. J. Remote Sens.* **29**, 17-18, 4961-4991, DOI: 10.1080/01431160802036516.

Su, Z. (2002), The Surface Energy Balance System (SEBS) for estimation of turbulent heat fluxes, *Hydrol. Earth Syst. Sci.* **6**, 1, 85-100, DOI: 10.5194/hess-6-85-2002.

Su, Z., T. Schmugge, W.P. Kustas, and W.J. Massman (2001), An evaluation of two models for estimation of the roughness height for heat transfer between the land surface and the atmosphere, *J. Appl. Meteor.* **40**, 1933-1951, DOI: 10.1175/1520-0450(2001)040<1933:AEOTMF>2.0.CO;2.

Su, Z., W. Timmermans, A. Gieske, L. Jia, J.A. Elbers, A. Olioso, J. Timmermans, R. van der Velde, X. Jin, H. van der Kwast, D. Sabol, J.A. Sobrino, J. Moreno, and R. Bianchi (2008), Quantification of land-atmosphere exchanges of water, energy and carbon dioxide in space and time over the heterogeneous Barrax site, *Int. J. Remote Sens.* **29**, 17-18, 5215-5235, DOI: 10.1080/01431160802326099.

Sun, S.F. (1982), Moisture and heat transport in a soil layer forced by atmospheric conditions, M.Sc. Thesis, University of Connecticut, Storrs.

Thom, A.S. (1975), Momentum, mass and heat exchange of plant communities. **In:** J.L. Monteith (ed.), *Vegetation and Atmosphere*, Academic Press, London, 57-110.

Timmermans, W.J., W.P. Kustas, M.C. Anderson, and A.N. French (2007), An intercomparison of the Surface Energy Balance Algorithm for land (SEBAL) and the Two-Source Energy Balance (TSEB) modeling schemes, *Remote Sens. Environ.* **108**, 4, 369-384, DOI: 10.1016/j.rse.2006.11.028.

Timmermans, W.J., Z. Su, and A. Olioso (2009), Footprint issues in scintillometry over heterogeneous landscapes, *Hydrol. Earth Syst. Sci.* **13**, 11, 2179-2190, DOI: 10.5194/hess-13-2179-2009.

Timmermans, W.J., J.C. Jiménez-Muñoz, V. Hidalgo, K. Richter, J.A. Sobrino, G. D'Urso, F. Mattia, G. Satalino, E. De Lathauwer, and V.R.N. Pauwels (2011), Estimation of the spatially distributed surface energy budget for AgriSAR 2006, Part I: Remote sensing model intercomparison, *JSTARS-IEEE* **4**, 2, 465-481, DOI: 10.1109/JSTARS.2010.2098019.

Timmermans, W., C. van der Tol, J. Timmermans, M. Ucer, X. Chen, L. Alonso, J. Moreno, A. Carrara, R. Lopez, F. de la Cruz Tercero, H.L. Corcoles, E. de Miguel, J.A.G. Sanchez, I. Pérez, B. Franch, J.-C.J. Munoz, D. Skokovic, J. Sobrino, G. Soria, A. MacArthur, L. Vescovo, I. Reusen, A. Andreu, A. Burkart, C. Cilia, S. Contreras, C. Corbari, J.F. Calleja, R. Guzinski, C. Hellmann, I. Herrmann, G. Kerr, A.-L. Lazar, B. Leutner, G. Mendiguren, S. Nasilowska, H. Nieto, J. Pachego-Labrador, S. Pulanekar, R. Raj, A. Schikling, B. Siegmann, S. von Bueren, and Z.B. Su (2015), An overview of the Regional Experiments For Land-atmosphere Exchanges 2012 (REFLEX 2012) campaign, *Acta Geophys.* **63**, 6, 1465-1484, DOI: 10.2478/s11600-014-0254-1 (this issue).

Twine, T.E., W.P. Kustas, J.M. Norman, D.R. Cook, P.R. Houser, T.P. Meyers, J.H. Prueger, P.J. Starks, and M.L. Wesely (2000), Correcting eddy-covariance flux underestimates over a grassland, *Agr. Forest Meteorol.* **103**, 3, 279-300, DOI: 10.1016/S0168-1923(00)00123-4.

van der Tol, C. (2012), Validation of remote sensing of bare soil ground heat flux, *Remot. Sens. Environ.* **121**, 275-286, DOI: 10.1016/j.rse.2012.02.009.

van der Tol, C., W.J. Timmermans, C. Corbari, A. Carrara, J. Timmermans, and Z. Su (2015), An analysis of turbulent heat fluxes and the energy balance during the REFLEX campaign, *Acta Geophys.* **63**, 6, 1516-1539, DOI: 10.1515/acgeo-2015-0061 (this issue).

Verhoef, A., B.J.J.M. van den Hurk, A.F.G. Jacobs, and B.G. Heusinkveld (1996), Thermal soil properties for vineyard (EFEDA-I) and savanna (HAPEX-Sahel) sites, *Agr. Forest Meteorol.* **78**, 1-2, 1-18, DOI: 10.1016/0168-1923(95)02254-6.

Wang, T., G.R. Ochs, and S.F. Clifford (1978), A saturation-resistant optical scintillometer to measure C^2_n, *J. Opt. Soc. Am.* **68**, 3, 334-338, DOI: 10.1364/JOSA.68.000334.

Wilson, K., A. Goldstein, E. Falge, M. Aubinet, D. Baldocchi, P. Berbigier, C. Bernhofer, R. Ceulemans, H. Dolman, C. Field, A. Grelle, A. Ibrom, B.E. Law, A. Kowalski, T. Meyers, J. Moncrieff, R. Monson, W. Oechel, J. Tenhunen, S. Verma, and R. Valentini (2002), Energy balance closure at FLUXNET sites, *Agr. Forest Meteorol.* **113**, 1-4, 223-243, DOI: 10.1016/S0168-1923(02)00109-0.

Wood, E.F., D.P. Lettenmaier, X. Liang, D. Lohmann, A. Boone, S. Chang, F. Chen, Y. Dai, R.E. Dickinson, Q. Duan, M. Ek, Y.M. Gusev, F. Habets, P. Irannejad, R. Koster, K.E. Mitchel, O.N. Nasonova, J. Noilhan, J. Schaake, A. Schlosser, Y. Shao, A.B. Shmakin, D. Verseghy, K.Warrach, P. Wetzel, Y. Xue, Z.-L. Yang, and Q. Zeng (1998), The Project for Intercomparison of Land-surface Parameterization Schemes (PILPS) Phase 2(c) Red-Arkansas river basin experiment: 1. Experiment description and summary intercomparisons, *Global Planet. Change* **19**, 1-4, 115-135, DOI: 10.1016/S0921-8181(98)00044-7.

Received 31 January 2014
Received in revised form 19 September 2014
Accepted 26 September 2014